Al-Azawi, Anas; Horenz, Christoph; Tupasela, Topi; Ikkala, Olli; Jokinen, Ville; Franssila, Sami; Ras, Robin H. A.

Slippery and magnetically responsive micropillared surfaces for manipulation of droplets and beads

Published in:
AIP Advances

DOI:
10.1063/5.0012852

Published: 01/08/2020

Document Version
Publisher's PDF, also known as Version of record

AIP Advances

Slippery and magnetically responsive micropillared surfaces for manipulation of droplets and beads

Cite as: AIP Advances **10**, 085021 (2020); https://doi.org/10.1063/5.0012852
Submitted: 05 May 2020 . Accepted: 29 July 2020 . Published Online: 17 August 2020

Anas Al-Azawi, Christoph Hörenz, Topi Tupasela, Olli Ikkala, Ville Jokinen, Sami Franssila, and Robin H. A. Ras

Slippery and magnetically responsive micropillared surfaces for manipulation of droplets and beads

Cite as: AIP Advances 10, 085021 (2020); doi: 10.1063/5.0012852
Submitted: 5 May 2020 • Accepted: 29 July 2020 •
Published Online: 17 August 2020 • Publisher Error Corrected: 19 August 2020

Anas Al-Azawi,[1] Christoph Hörenz,[1] Topi Tupasela,[1] Olli Ikkala,[1,2] Ville Jokinen,[3] Sami Franssila,[3] and Robin H. A. Ras[1,2,a)]

AFFILIATIONS

[1]Department of Applied Physics, Aalto University, P.O. Box 15100, FI-00076 Aalto, Espoo, Finland
[2]Department of Bioproducts and Biosystems, Aalto University, P.O. Box 15100, FI-00076 Aalto, Espoo, Finland
[3]Department of Chemistry and Materials Science, Aalto University, P.O. Box 13500, FI-00076 Aalto, Espoo, Finland

[a)]**Author to whom correspondence should be addressed:** robin.ras@aalto.fi

ABSTRACT

Stimuli-responsive surfaces are of practical importance for applications ranging from enhanced mixing of reagents in lab-on-a-chip systems until probing cellular traction forces. Non-destructive reversible bending of cilia-inspired magnetic pillars can be used for controlled transportation of non-magnetic objects and bio-inspired sensing. Magnetic actuation of micropillars suspended in liquids allows controlled mixing, propelling, and stirring of fluids as well as droplet manipulation, which are important for various applications including generation of cell spheroids and droplet coalescence in microfluidic systems. In order to expand their practical applications, fabrication processes capable of rapid prototyping have to be developed. Inspired by biological cilia and their functionalities, actuating hairy surfaces are herein fabricated and implemented to manipulate both microbeads and droplets. The artificial cilia are based on microscale magnetic pillar arrays made of flexible polydimethylsiloxane functionalized with magnetic microparticles. The arrays are fabricated by a new method using patterned molds that relies on cryogenic separation to produce transparent cilia-inspired arrays without requiring manual interference to clean the templates during the process. Magnetic actuation of the pillar arrays is demonstrated in isopropanol and silicone oil. Filling with oil yields magnetically responsive slippery lubricated surfaces allowing directional motion of droplets by repetitive bending and recovery of the flexible magnetic pillars. The achieved structures allow manipulation of microbeads and droplets which is uncommon even at the sub-mm scale; directional motion is demonstrated for 250 μm–550 μm sized droplets. Droplet transportation is facilitated by extremely low hysteresis and a high degree of omnidirectional bending of the pillar array.

I. INTRODUCTION

Dynamic and anisotropic high-aspect ratio (AR) micro-/nanostructures confer essential functionalities in both biological and man-made surfaces. Cilia structures present in the respiratory passage epithelia surface are responsible for clearance of mucus and pathogens.[1,2] Induced propulsive and rotational flow of motile cilia allows vital and diverse fluid mediated processes in biological systems, such as biochemical signaling and sensing.[3,4] Artificial cilia are, therefore, envisaged as a biomimetic strategy to achieve fluid manipulation at the microscale.

Droplet manipulation by microscale ciliary structures has potential applications in microfluidic systems,[5–7] emulsion separation,[8] and dynamic interfacing with biomatter.[9,10] Spontaneous and directional droplet transport has been demonstrated by designing surfaces with wettability gradients.[11–15] This passive mechanism for achieving droplet motion is limited by the irreversible nature of the unidirectional motion dictated by the fixed structure/wettability gradient. Alternatively, dynamic responsive structured surfaces provide direct control of the structure pattern by applying external stimuli. Magnetic microstructures offer an attractive route for droplet

manipulation because of the reversible actuation, instantaneous response, and the non-invasive nature of the magnetic field, also allowing remote control of the surface properties.

Cilia-inspired magnetic micro-/nanostructures have generated considerable interest resulting in several possible fabrication techniques for the magnetically actuated surfaces. Bottom-up approaches for the formation of magnetic cilia-like structures from a suspension of magnetic particles and a prepolymer in an external magnetic field have been demonstrated and utilized for droplet manipulation.[16–20] Such a template-free technique relies on the alignment of the magnetic particles in the prepolymer as a response to an applied magnetic field. The lack of precise control of the length scale and pattern design of such cilia-like pillars is a potential obstacle for the integration and application of surfaces produced by this method.

Polycarbonate track etched (PCTE) membranes have been utilized for the production of electroplated nickel pillars with spherical caps and polydimethylsiloxane (PDMS) cilia-like magnetic pillars.[21,22] Using PCTE membranes for replication of the magnetic microstructures allowed control over pattern parameters, such as diameter, aspect ratio, and pillar density; however, the random location of the holes across the membrane and the subsequent position of the pillars are expected to involve an adverse effect on the functionality. Successful application of the magnetic ciliary structure toward controlled liquid manipulation requires uniform distribution of the cilia structures within the patterned area as random distribution can cause irregularities in fluid manipulation. Arrays of magnetic micropillars with controlled length and spacing have previously been generated by microlithography combined with replica molding.[23–26] Therein, PDMS has been established as the preferred material for the synthesis of actuating cilia-mimics inspired by the magnetic microstructures based on the rapid prototyping, biocompatibility, transparency, and elasticity.[27,28] Several strategies have been developed to achieve droplet motion on PDMS pillared surfaces, such as magnetically controlled bending of the magnetic pillars assisted with vibration.[26] Another procedure is generation of a local area of bent magnetic pillars on which droplets can be moved by controlling the location of a permanent magnet beneath the sample.[18,29]

To overcome the challenges of the application and integration of the magnetic cilia-inspired structures, it is important to develop a fabrication process that meets several criteria. First, the magnetic cilia should be replicated from a disposable mold of a predefined pattern definition that is designed according to an intended functionality. Second, only the micropillars or the cilia-like structures should be magnetic to enable magnetic actuation of the pillars alone and not the sample as a whole. This is beneficial for practical applications, such as dynamically controlling light transmittance. Finally, the fabrication process must be repeatable, and the design layout should not hinder or alter the implementation of the fabrication steps.

Previous attempts for achieving water droplet manipulation by magnetic actuation relied mainly on either modifying the pillar surface with a secondary structure of low surface energy to achieve superhydrophobicity[18,26] or infusing lubricants to the surface structure.[29] Recently, we demonstrated water droplet motion by the repetitive bending and recovery of superhydrophobic thiol–ene micropillars decorated by colloidal micro- and nanoparticles.[30] Super water-repellency can also be achieved by infusing lubricant to lower the surface energy. However, directional and controlled droplet motion remains a challenge, especially at the sub-mm scale where droplet motion by repetitive bending and recovery of slippery lubricant infused arrays of PDMS micropillars has not been explored.

Inspired by cilia, we present responsive surfaces based on a micropillar/magnetic particle composite by a simple new approach involving cryogenic separation of a structured PDMS template from a magnetic layer. We demonstrate instantaneous response of the magnetic pillars to the magnetic field while the sample is immersed in isopropanol or silicone oil. Swelling of the PDMS magnetic pillars in silicone oil led to slippery arrays showing reduced contact angle hysteresis (CAH). Controlled omnidirectional motion of water droplets by repetitive bending and recovery of the magnetic pillars is demonstrated. Additionally, the magnetic micropillar array is capable of microbead motion.

II. FABRICATION

Fabrication of the magnetically responsive surfaces starts by preparing two types of silicon pillar array masters by photolithography and deep reactive ion etch (DRIE) (see Fig. S1, supplementary material). The low aspect ratio silicon pillar diameter is 9.1 μm, and the height is 46 μm, whereas the diameter and the height of the high aspect ratio pillars are 8.5 μm and 68.8 μm, respectively. In both cases, the pitch is 30 μm. The masters were subsequently used to prepare PDMS templates with hollow cavities [Fig. 1(a)]. Such PDMS templates were then silanized followed by application of uncured PDMS containing 50 wt. % of superparamagnetic magnetic carbonyl iron particles (CIP) (BASF SE, Grade CIP HS) with a size distribution of 600 nm–3.0 μm onto the template [Figs. 1(b) and S2]. Afterward, the PDMS template was placed on top of a permanent magnet. Next, a flat backing layer of cured PDMS was placed on top of the uncured CIP-PDMS composite layer, and the assembly was left on a fixed distance above the permanent magnet. Subsequently, the assembly of the flat PDMS backing layer, the PDMS template, and the uncured CIP-PDMS layer sandwiched between them was cured in an oven [Fig. 1(c)]. The flat backing layer of cured PDMS shown in Fig. 1(c) compensates for the use of a thick layer of PDMS mixed with CIP that is contained within the borders of the template during the fabrication process steps. After curing, the assembly was soaked in liquid nitrogen, and the mismatch in thermal expansion coefficients between the PDMS template and the PDMS containing magnetic CIP caused cleavage at the interface with the template [Fig. 1(d) and Fig. S3]. This method yields the cavities of the PDMS template filled with the cured PDMS containing CIP after separation. A new layer of uncured PDMS acting as the substrate layer was applied onto the template. In contrast to the surface of the PDMS template, the CIP-PDMS composite was not silanized. Thus, the substrate layer only binds to PDMS embedded with CIP after curing [Fig. 1(e)]. The magnetic pillar array was then manually separated from the template in ethanol [Fig. 1(f)].

Inspections of PDMS templates after the cryogenic separation step by optical microscopy [Fig. 1(g)] and scanning electron microscopy (SEM) shown in Fig. S4 confirm the confinement of CIP within the cavities of the PDMS template. Immersing the sample,

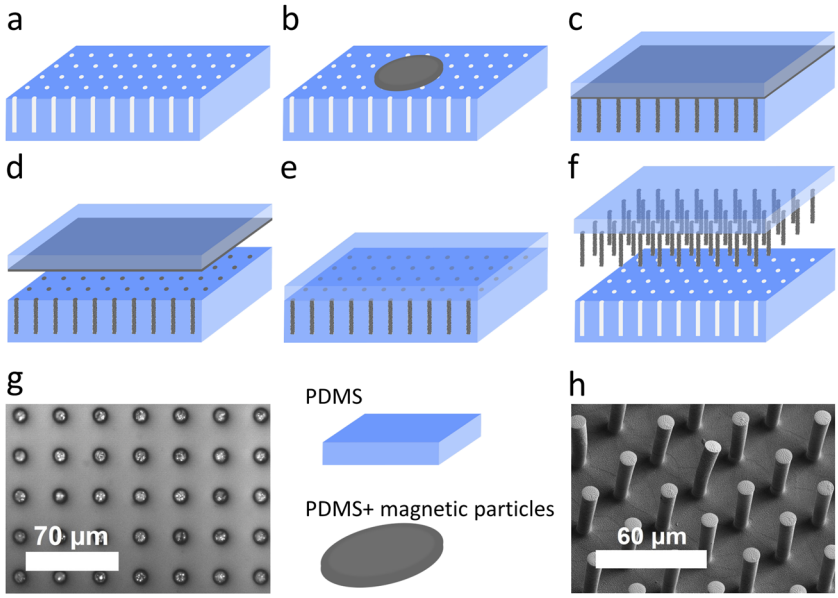

FIG. 1. Fabrication process steps for producing PDMS/magnetic particle pillars. (a) PDMS template obtained from the etched silicon master and treated with a low energy self-assembled monolayer. (b) Depositing PDMS mixed with magnetic particles and the use of a permanent magnet for magnet-assisted filling of the cavities. (c) Flat backing layer of cured PDMS is placed on top of the PDMS layer embedded with magnetic particles, and the assembly is cured in the oven. (d) Immersing in liquid nitrogen causes cleavage of the cured PDMS layer containing magnetic particles at the interface with the template. The separation yields the mold cavities filled with cured PDMS containing magnetic particles. (e) Application of a PDMS layer to the template followed by curing to form the substrate layer. (f) Demolding the magnetic PDMS pillar array in ethanol. (g) PDMS mold characterization by optical microscopy after liquid nitrogen separation reveals the confinement of the magnetic material within the cavities of the template. (h) SEM image of the magnetic PDMS pillar array after freeze drying.

after the demolding step, in water followed by freeze drying enables SEM visualization of the magnetic micropillar array [Fig. 1(h)].

Introducing cryogenic separation in the fabrication process of the magnetic pillars offers several advantages including preparation of clean templates where magnetic particles are confined within the cavities only resulting in transparent samples after the second replication. In particular, this process eliminates the need for scraping the excess of the magnetic particles away from the surface of the template, unlike in previous reports where particle contamination was manually removed from the mold.[23,25,31] In some cases, the residual magnetic layer was not removed,[26] while in the work of Ben *et al.*,[32] the mold was sacrificed in 24 h dissolving process step. In addition, the same PDMS template can be used multiple times improving the efficiency for the replication of the magnetic pillar array.

The fabrication process can be applied for the fabrication of microfluidic systems with the magnetic pillars integrated in a channel segment. This cannot be realized with the bottom-up approach.

III. EXPERIMENTAL

Two types of pillar arrays, distinguished by the value of aspect ratio (AR), are produced from the two silicon masters. PDMS magnetic pillars replicated from the first silicon master [Fig. S1(a)] have an AR equal to 4.8 (Fig. S5). The value of AR of pillars replicated from the second silicon master [Fig. S1(b)] is 8.8 as shown in Fig. S6(a). Given the array pitch value of 30 μm and the low Young's modulus of PDMS, it is necessary to keep the pillars immersed in isopropanol or oil during application to avoid capillary force induced collapse of the pillars [Fig. S6(b)].[33–35] The magnetic pillars can be recovered from the collapsed state to the functioning state by sonication.

Actuation of the pillars was achieved by bringing a permanent magnet to the vicinity of the bottom of the sample [Fig. 2(a)]. The magnitude and direction of pillar bending are determined by the strength and the direction of the magnetic flux density by manually adjusting the orientation and the gap of the magnet movement relative to the sample. Actuation was performed both in isopropanol and in silicone oil [Figs. 2(b) and 2(c), Movie 1 (Multimedia view), and Movie 2 (Multimedia view)].

Next, the pillar flexibility in isopropanol and silicone oil is demonstrated. The degree of swelling of PDMS in water, isopropanol, and most alcohols is low with a swelling ratio ($S_W = D/D_0$) ranging from 1 to 1.09, where D is the length of a PDMS segment in the solvent and D_0 is the segment length of dry PDMS.[36] The swelling of the pillar dimensions in silicone oil is 30.7% corresponding to $S_W = 1.31$, confirmed for both PDMS magnetic pillars of aspect ratios 4.8 and 8.8 [Figs. 2(d) and 2(e), Movie 3 (Multimedia view), Movie 4 (Multimedia view), and Fig. S7].

Young's modulus measurements conducted using a mechanical tester on PDMS embedded with CIP (50 wt. % CIP) before and after oil immersion confirmed the change in elastic properties. The measured value of Young's modulus increased from 2.05 ± 0.20 MPa before oil immersion to 3.38 ± 0.41 MPa after oil immersion

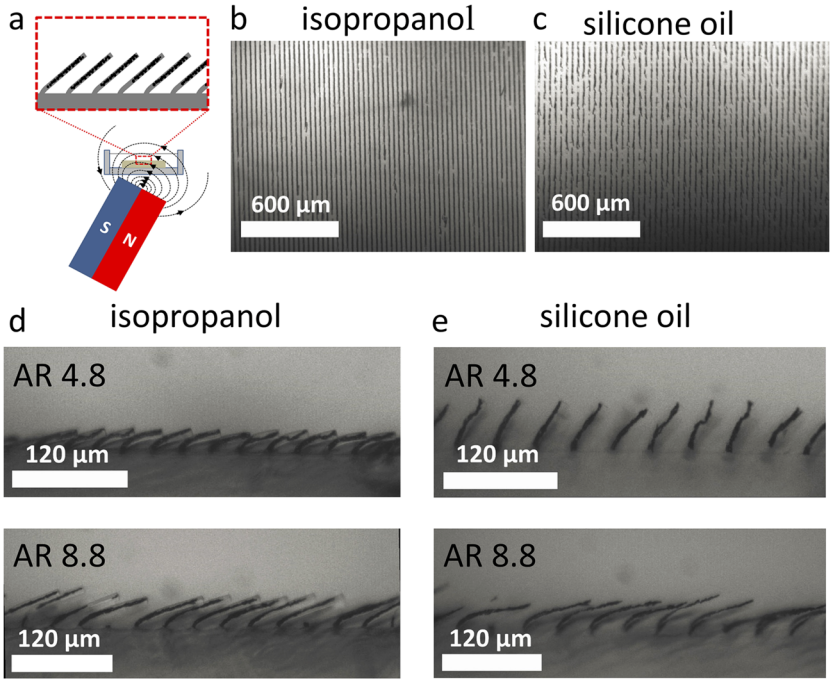

FIG. 2. Actuation of magnetic pillars using a permanent magnet. (a) Sketch illustrating the procedure of PDMS magnetic pillar bending. Snapshot images of videos recorded by optical microscopy showing top view of 8.8 AR magnetic pillars immersed in isopropanol (b) and silicone oil (c) during actuation. Snapshot images of recorded movies displaying side views of the pillar array bending in isopropanol (d) and silicone oil (e). Multimedia views: (b) https://doi.org/10.1063/5.0012852.1; (c) https://doi.org/10.1063/5.0012852.2; (d) https://doi.org/10.1063/5.0012852.3; and (e) https://doi.org/10.1063/5.0012852.4

[Fig. S8(a)]. The measured value of Young's modulus of PDMS without embedded CIP is 1.59 ± 0.05 MPa before oil immersion and 1.80 ± 0.13 MPa after oil immersion [Fig. S8(b)]. The change in elastic properties is also manifested by a decrease in the maximum bending of 4.8 AR pillars after oil immersion, as shown in Fig. 2(e) (Multimedia view). Assuming point load at the free end of the pillars, the relation between force F and pillar deflection δ is given as

$$F = \left(3EI/h^3\right)\delta.^{37} \quad (1)$$

Hence, magnetic pillars of 8.8 AR require less force for large pillar deflection compared with the lower AR pillars that exhibit limited pillar deflection after oil immersion if subjected to the same magnetic field. Using an expression obtained from numerical modeling[38] for bending of micron sized PDMS posts that accounts for large deflection values, the relation between F and δ of PDMS pillars of Young's modulus of 3.38 MPa is estimated and shown in Fig. S9.

A high degree of pillar bending of the high AR pillars demonstrated in Fig. 2 (Multimedia view) is achieved with relatively low magnetic field strength (150 mT–200 mT). Actuation of 8.8 AR pillars did not exhibit overlap between adjacent pillars or limited bending. This enables sufficient force to be generated for successful application of the magnetic pillar array in fluid manipulation.

Lubricating the PDMS micropillars in oil affects the surface as well as elastic properties of the magnetic pillars. Swelling of the magnetic pillars in silicone oil results in a slippery lubricant infused surface without compromising omnidirectional bending and large deflection of 8.8 AR pillars despite a noticeable increase in Young's modulus after oil immersion. A water droplet deposited on the pillar array is suspended in the Cassie state on the oil infused structure. Manual control of the magnet movement beneath the sample is done in a way that the pillars experience bending followed by recovery resulting from the elastic restoring force acting on the deflected pillars when the magnetic field gradient is directed away from the sample. By repeating the cycle of bending and recovery, droplet motion is initiated along the beating direction of the magnetic pillars [Fig. 3, Movie 5 (Multimedia view), and Movie 6 (Multimedia view)].

Non-wettability acquired by oil immersion is obvious from water droplets beading up. On a flat PDMS that has not been exposed to oil, the measured advancing contact angle is 115.4°, and the receding contact angle is 100.8° (Fig. S10). In comparison, the mean values for both the advancing and receding contact angles are 171.4° measured on the surface of the magnetic pillars immersed in silicone oil (Fig. S11). Furthermore, impinging the magnetic PDMS pillars with a 2 μl water droplet attached to a needle moving at a velocity of 10 mm/min followed by retracting the droplet upward away from the surface caused neither droplet transition to the Wenzel state nor pillar collapse noticed after droplet extraction (Fig. S12 and Movie S1, supplementary material).

Water droplet motion at the sub-mm scale was enabled by exerting force onto the droplet using the repeated bending and recovery mechanism. The motion of a water droplet on the magnetic pillar array immersed in oil is depicted by the relation based on Newton's second law, as shown in Eq. (2),

$$\rho V\left(\partial^2 x/\partial t^2\right) = F_{\text{pillars}} + F_{\text{CAH}} + F_{\text{d}}, \quad (2)$$

where ρ is the density, V is the volume of the droplet, and F_{pillars} is the actuating force of the pillars. The actuation force of a single pillar is given by Eq. (1). Forces that oppose droplet motion are the drag force (F_{d}) and the friction force (F_{CAH}) resulting from CAH of the micropillared surface. These forces are expressed as follows:

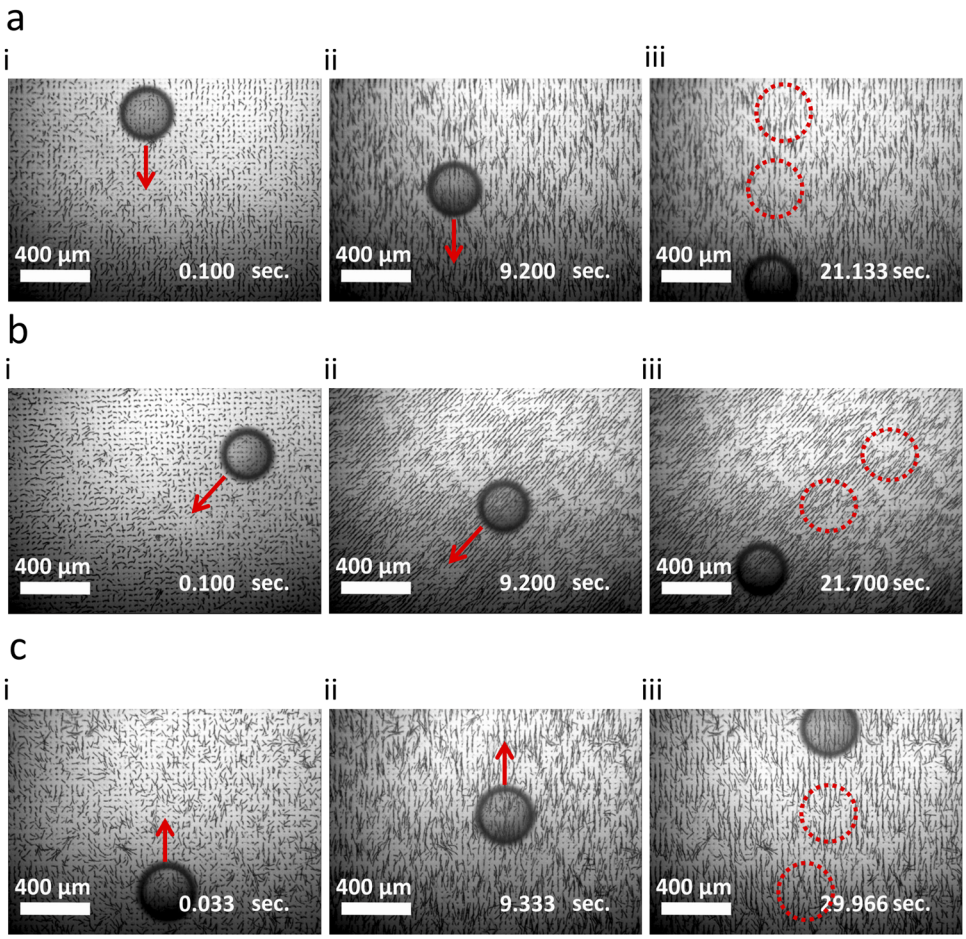

FIG. 3. Snapshot images of recorded movies showing top view of controlled water droplet motion enabled by the repeated bending and recovery of the slippery PDMS magnetic pillars in silicone oil. (a)–(c) Directional droplet motion along three different straight paths. Multimedia views: (a) https://doi.org/10.1063/5.0012852.5; (c) https://doi.org/10.1063/5.0012852.6

$$F_d = -2\pi\eta_o r v(3 + 2\lambda/1 + \lambda), \quad (3)$$

where η_o is the viscosity of oil, r is the droplet radius, v is the droplet velocity, and $\lambda = \eta_o/\eta_w$; η_w is the viscosity of water. The CAH force is

$$F_{CAH} = -\left(24/\pi^3\right) D_w \gamma(\cos\theta_R - \cos\theta_A), \quad (4)$$

where D_w is the base diameter of the droplet, γ is the surface tension of the water–oil interface, θ_R is the receding contact angle, and θ_A is the advancing contact angle.

The slippery oil infused pillars exhibit negligible CAH and F_{CAH}. As a result, initiating droplet motion is dictated by the actuating force ($F_{pillars}$), which is provided by pillar bending and recovery.

To the best of our knowledge, magnetic structures have been mainly used to demonstrate handling of large non-magnetic droplets (few microliters in volume) according to previous reports.[7,16,18–20,23,26,29] To initiate directional motion of ≈286 μm wide droplet (corresponding volume ≈0.01 μl), as shown in Fig. 3 (Multimedia view), the force provided by collective actuation of pillars must exceed $F_{CAH} + F_d$. This is accomplished by ensuring

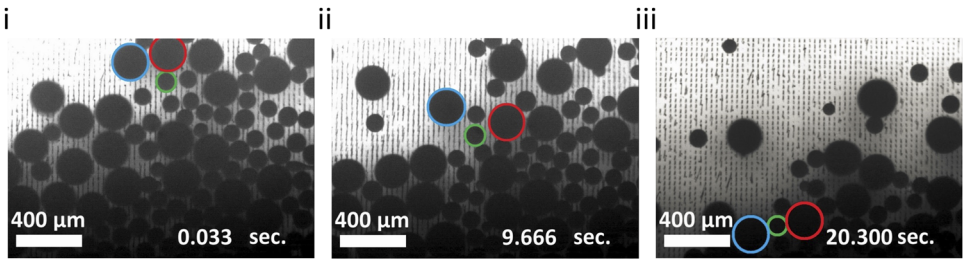

FIG. 4. Snapshot images of a recorded movie demonstrating the ability of polyethylene microbead transport by the magnetic micropillars in isopropanol. Time elapsed 20.3 s. Three beads are highlighted to keep track on the directed bead motion during collective pillar actuation. Multimedia views: (i) https://doi.org/10.1063/5.0012852.7; (ii) https://doi.org/10.1063/5.0012852.8

powerful bending actuation at relatively low magnetic field strength of high AR micropillars combined with extremely low CAH. Apart from surface defects that can temporarily impede droplet motion, droplet motion at a velocity of ≈2.75 mm/min is achieved along different paths.

Inserting parameters obtained from Fig. 3 (Multimedia view), such as the average velocity and the radius of the droplet, into Eq. (3) yields $F_d = -0.409$ nN. In comparison, the actuating force of a single pillar is $F_{pillar} = 0.414$ μN, which is calculated by Eq. (1) for a pillar deflection (δ) value of 50 μm estimated from bending of a pillar of AR = 8.8 in oil [Fig. 2 (Multimedia view)] and using $E = 3.38$ MPa, $h = 69$ μm, and $d = 8.6$ μm, which represent the elastic modulus, height, and diameter, respectively. During actuation, multiple pillars acting on the three-phase contact line and, thus, the actuating force exceed the opposing forces enabling controlled droplet motion by repetitive bending and recovery of the micropillars.

In addition to water, the motion of a glycerol droplet is also demonstrated by the repetitive bending and recovery of the slippery PDMS magnetic pillars (Fig. S13 and Movie S2, supplementary material).

Next, polyethylene microbeads of two size distributions 106 μm –125 μm and 212 μm–250 μm are mixed together in isopropanol and pipetted on the sample immersed in isopropanol. The density of the microbeads is 1.2 g cm^{-3}, which is higher than that of isopropanol, so the beads sediment on top of the pillared surface and can be directed by the actuation of the pillars. Directional transport of microbeads along the surface was also induced by the repetitive bending and recovery of the magnetic pillars [Fig. 4, Movie 7 (Multimedia view), Movie 8 (Multimedia view), and Fig. S14)].

IV. CONCLUSIONS

In this work, we present a novel technique to fabricate a dense set of PDMS magnetic micropillars that translate magnetic actuation to fluid and microbead manipulation. The magnetic pillar arrays demonstrate fast response and cilia-like beating enabled directional and continuous small-size water droplet motion in silicone oil. The liquid infused layer reduces CAH to the point where the surface exhibits no pinning. In addition, polyethylene microbead transport in isopropanol was demonstrated by the micropillar array.

We envision that magnetic pillars integrated in microfluidic systems can be realized by implementing the same fabrication steps with different mold designs that take into account the desired application of the pillars within the system whether it is mixing, manipulation, or controlling the passage of micro-objects. This work can streamline the production of cilia-like patterns of various geometrical shapes and dimensions.

SUPPLEMENTARY MATERIAL

See the supplementary material for detailed description of the fabrication process, characterization of the template and the pillars by scanning electron microscopy, Young's modulus measurements of the PDMS–magnetic particle composite before and after oil immersion, wettability characterization of oil infused PDMS magnetic pillars, and glycerol droplet motion.

ACKNOWLEDGMENTS

This work was supported by the European Research Council, Grant No. ERC-2016-CoG (725513-SuperRepel), and the Academy of Finland [Centers of Excellence Programme (2014-2019) and Project Nos. 256206, 266820, and 297360]. This work made use of the Aalto University Nanomicroscopy Center and the cleanroom facilities of the Micronova Nanofabrication Center. The authors would like to thank BASF for generously providing the magnetic particles.

DATA AVAILABILITY

The data that support the findings of this study are available from the corresponding author upon reasonable request.

REFERENCES

[1] B. Button, L.-H. Cai, C. Ehre, M. Kesimer, D. B. Hill, J. K. Sheehan, R. C. Boucher, and M. Rubinstein, Science **337**, 937 (2012).
[2] A. S. Shah, B. S. Yehuda, T. O. Moninger, J. N. Kline, and M. J. Welsh, Science **325**, 1131 (2009).
[3] P. Satir and S. T. Christensen, Annu. Rev. Physiol. **69**, 377 (2006).
[4] D. Chen, D. Norris, and Y. Ventikos, Med. Eng. Phys. **33**, 857 (2011).
[5] J. Belardi, N. Schorr, O. Prucker, and J. Rühe, Adv. Funct. Mater. **21**, 3314 (2011).
[6] J. M. J. den Toonder and P. R. Onck, Trends Biotechnol. **31**, 85 (2013).
[7] Y. Zhou, S. Huang, and X. Tian, Adv. Funct. Mater. **30**, 1906507 (2020).
[8] K. Li, J. Ju, Z. Xue, J. Ma, L. Feng, S. Gao, and L. Jiang, Nat. Commun. **4**, 2276 (2013).
[9] R. M. Judith, J. K. Fisher, R. C. Spero, B. L. Fiser, A. Turner, B. Oberhardt, R. M. Taylor, M. R. Falvo, and R. Superfine, Lab Chip **15**, 1385 (2015).
[10] N. J. Sniadecki, A. Anguelouch, M. T. Yang, C. M. Lamb, Z. Liu, S. B. Kirschner, Y. Liu, D. H. Reich, and C. S. Chen, Proc. Natl. Acad. Sci. U. S. A. **104**, 14553 (2007).
[11] Z. Guo and J. Li, Nanoscale **10**, 13814 (2018).
[12] J. Li, X. Tian, A. P. Perros, S. Franssila, and V. Jokinen, Adv. Mater. Interfaces **1**, 1400001 (2014).
[13] J. Li, Q. H. Qin, A. Shah, R. H. A. Ras, X. Tian, and V. Jokinen, Sci. Adv. **2**, e1600148 (2016).
[14] S. Huang, J. Li, L. Liu, L. Zhou, and X. Tian, Adv. Mater. **31**, 1901417 (2019).
[15] Y. Wang, K. Ma, and J. H. Xin, Adv. Funct. Mater. **28**, 1705128 (2018).
[16] J. V. I. Timonen, C. Johans, K. Kontturi, A. Walther, O. Ikkala, and R. H. A. Ras, ACS Appl. Mater. Interfaces **2**, 2226 (2010).
[17] Y. Wang, Y. Gao, H. Wyss, P. Anderson, and J. den Toonder, Lab Chip **13**, 3360 (2013).
[18] J. H. Kim, S. M. Kang, B. J. Lee, H. Ko, W. G. Bae, K. Y. Suh, M. K. Kwak, and H. E. Jeong, Sci. Rep. **5**, 17843 (2015).
[19] M. Cao, X. Jin, Y. Peng, C. Yu, K. Li, K. Liu, and L. Jiang, Adv. Mater. **29**, 1606869 (2017).
[20] C. Yang, L. Wu, and G. Li, ACS Appl. Mater. Interfaces **10**, 20150 (2018).
[21] A. Grigoryev, I. Tokarev, K. G. Kornev, I. Luzinov, and S. Minko, J. Am. Chem. Soc. **134**, 12916 (2012).
[22] A. R. Shields, B. L. Fiser, B. A. Evans, M. R. Falvo, S. Washburn, and R. Superfine, Proc. Natl. Acad. Sci. U. S. A. **107**, 15670 (2010).
[23] D.-M. Drotlef, P. Blümler, P. Papadopoulos, and A. Del Campo, ACS Appl. Mater. Interfaces **6**, 8702 (2014).
[24] D.-M. Drotlef, P. Blümler, and A. Del Campo, Adv. Mater. **26**, 775 (2014).
[25] B. Zhou, W. Xu, A. A. Syed, Y. Chau, L. Chen, B. Chew, O. Yassine, X. Wu, Y. Gao, J. Zhang, X. Xiao, J. Kosel, X.-X. Zhang, Z. Yao, and W. Wen, Lab Chip **15**, 2125 (2015).
[26] Y. Lin, Z. Hu, M. Zhang, T. Xu, S. Feng, L. Jiang, and Y. Zheng, Adv. Funct. Mater. **28**, 1800163 (2018).

[27]G. M. Whitesides and J. C. McDonald, Acc. Chem. Res. **35**, 491 (2002).
[28]A. A. S. Bhagat, P. Jothimuthu, and I. Papautsky, Lab Chip **7**, 1192 (2007).
[29]S. Ben, T. Zhou, H. Ma, J. Yao, Y. Ning, D. Tian, K. Liu, and L. Jiang, Adv. Sci. **6**, 1900834 (2019).
[30]A. Al-Azawi, Z. Cenev, T. Tupasela, B. Peng, O. Ikkala, Q. Zhou, V. Jokinen, S. Franssila, and R. H. A. Ras, Macromol. Rapid Commun. **41**, 1900522 (2019).
[31]Z. Yang, J. K. Park, and S. Kim, Small **14**, 1702839 (2017).
[32]S. Ben, J. Tai, H. Ma, Y. Peng, Y. Zhang, D. Tian, K. Liu, and L. Jiang, Adv. Funct. Mater. **28**, 1706666 (2018).
[33]D. Chandra and S. Yang, Langmuir **25**, 10430 (2009).
[34]J. Hansson, H. Yasuga, T. Haraldsson, and W. van der Wijngaart, Lab Chip **16**, 298 (2016).
[35]M. Kanungo, H. Lu, G. G. Malliaras, and G. B. Blanchet, Science **323**, 234 (2009).
[36]J. N. Lee, C. Park, and G. M. Whitesides, Anal. Chem. **75**, 6544 (2003).
[37]P. Papadopoulos, B.-E. Pinchasik, M. Tress, D. Vollmer, M. Kappl, and H.-J. Butt, Soft Matter **14**, 7429 (2018).
[38]Y. Xiang and D. A. LaVan, Appl. Phys. Lett. **90**, 133901 (2007).
[39]E. Guyon, J.-P. Hulin, L. Petit, and C. D. Mitescu, *Physical Hydrodynamics*, 2nd ed. (Oxford, 2015), pp. 331–337.
[40]A. I. ElSherbini and A. M. Jacobi, J. Colloid Interface Sci. **299**, 841 (2006).